RGNZ/MGPB

Late Quaternary activity of the Haramachi segment of the Futaba Fault in Northeast Japan through topographic anaglyph images and borehole core sediment analysis

Rudarsko-geološko-naftni zbornik
(The Mining-Geology-Petroleum Engineering Bulletin)
UDC: 550.8
DOI: 10.17794/rgn.2023.2.12
Original scientific paper

Anggraini Rizkita Puji[1]; Naoya Takahashi[2]; Shinji Toda[2]

[1] *Research Center for Geological Disaster, National Research and Innovation Agency, Jalan Sangkuriang, Bandung 40135, Indonesia*

[2] *Department of Earth Science, Tohoku University, 468-1, Aoba, Aoba-ku, Sendai, Miyagi, 980-8572, Japan*

Abstract

The Haramachi Fault segment in the northeastern part of Honshu Island, Japan, has mainly sinistral fault movements with minor reverse component within the Futaba Fault Zone in the northeastern Japan arc. The 2011 Mw 9.0 earthquake occurred off the Pacific coast of Tohoku which caused large crustal deformations. Despite being the closest active fault to the epicenter, very limited investigation has been conducted on the Futaba Fault Zone. Previous studies used smaller scale topographic maps and fault activity was estimated only from trenching and borehole investigations in the central part of the Haramachi Fault segment. Thus, geometry, kinematic, and recent tectonic activity of the fault segment is not well identified, especially in northern part. In this study, we use a combination of high-resolution DEMs (2-m and 5-m mesh), several types of topographic anaglyph images (slope, negative and positive openness), and conducted field survey to confirm remote sensing interpretation. Subtle surface expression of deformation associated with active faulting, such as deformed terrace risers, deflected drainages, and small fault scarps can now be identified more clearly. Several new fault strands in the northern part of the segment were found supported by fault outcrops found in the field confirming the recent activity of the fault system. *The new estimation of the total length of the Haramachi segment produced from the approach of this study yields 25 km, which is capable of producing Mw 6.5 – 7.0 or Mjma 7.2 earthquakes if ruptures were to occur altogether in the future.* Moreover, a shallow borehole survey and radiocarbon dating from the soil organic material has revealed the minimal timing estimation of the most recent faulting in the Haramachi segment to be 3694 ± 24 BP. This research provides a revised understanding of active fault distribution and deformation associated with the Haramachi segment and validates the timing of the most recent faulting event more broadly.

Keywords:
Late Quaternary activity; Haramachi segment; Futaba Fault Zone; Northeast Japan

1. Introduction

There is an increasing demand for a more reliable earthquake hazard mitigation in society. Every earthquake hazard is sourced from active fault movement, which largely depends on the geological, geophysical, and geodetic observation to analyze the active fault deformation in the crustal region. The refinement of the current hazard analysis is necessary to improve the attempt to reduce potential damage due to earthquakes. Using tectonic geomorphology has become a well-accepted method to evaluate evidence of active faulting, uplift, and folding near plate margins (**Keller et al., 1999; Burbank and Anderson, 2011**). The technique that utilizes geomorphic features to detect active tectonics has been implemented in different tectonic environments around the world, such as those with extensional faulting, slow convergence, or rapid convergence. The widespread adoption and versatility of this approach have been well-documented.

Corresponding author: Anggraini Rizkita Puji
e-mail address: anggra026@brin.go.id; anggrainirizkita@gmail.com

Geomorphological characteristics that typically arise from repeated earthquakes tend to create specific patterns that can be readily discerned through satellite images. With the support of high-definition DEM (Digital Elevation Model) and satellite imagery that recently has become more available and freely accessible, the reexamination of active faulting could reveal small scale but significant geomorphic features that may be used for challenging issues from previous studies. Thus, the new detailed investigation of tectonic geomorphology using such high-resolution methods could improve the estimation of potential earthquake hazards.

Large crustal deformations occurred in the northeast Japan arc during March 11, 2011, which caused an earthquake (Mw 9.0) with its epicenter off the Pacific coast of Tohoku that ruptured a 500-km long and 200-km wide megathrust (**Simons et al., 2011**) and produced a devastating 20-m-high tsunami (**Mori et al., 2011**). According to **Toda et al. (2011)**, the Mw 9 Tohoku earthquake resulted in a shift in the conditions for failure of the active faults across Japan, particularly the northeast Japan arc.

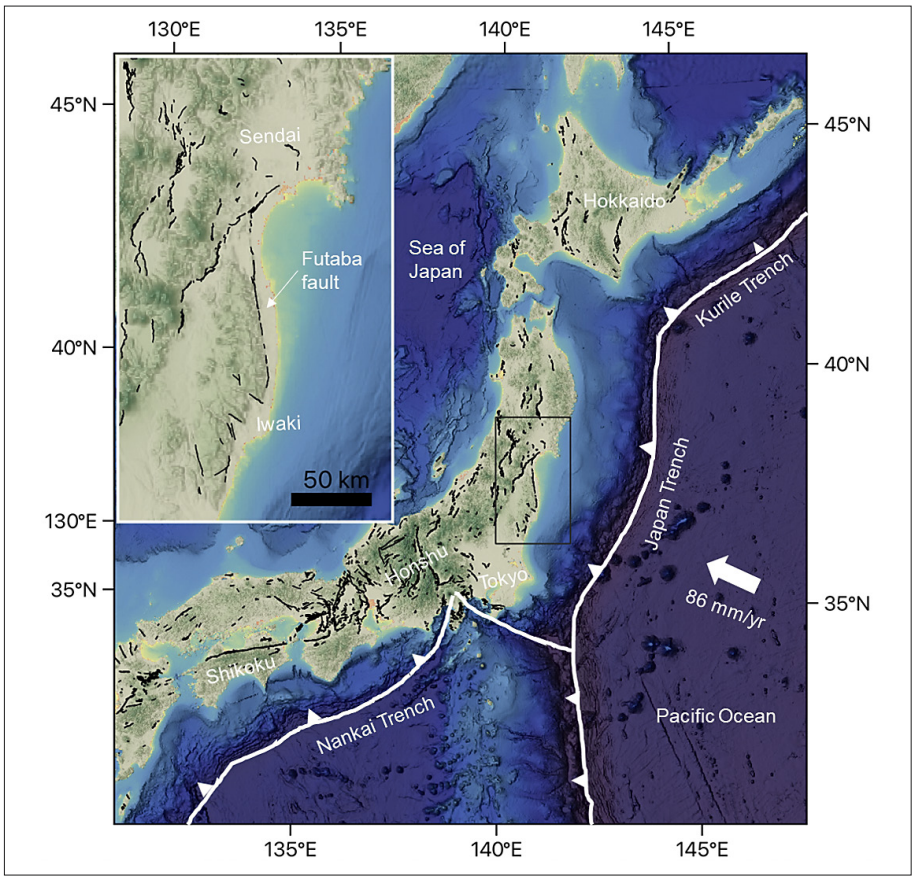

Figure 1: Shaded relief map of Japan (ETOPO2022) showing tectonic boundaries, location of the Futaba Fault, and active faults of Japan (black lines) (**Nakata and Imaizumi, 2002**).

In addition, the Headquarters for Earthquake Research Promotion conducted a long-term evaluation of active faults after the devastated event and have concluded that there are at least five major active fault zones with a high probability of earthquake occurrence, including the Futaba Fault Zone (**HERP, 2011**). Thus, this updated study is considered necessary to examine the active deformation thoroughly in order to understand its seismic risk and recent activity.

To date, the Futaba Fault Zone has been scarcely examined, therefore this study brings new results of this active fault zone. The most recent investigation of fault activity on the Futaba Fault relied on aerial photographs and topographic maps of a smaller scale, focused on the central part of the Haramachi segment (Tochikubo area) (**Kaneda et al., 2013; Fukushima-ken, 1999; Suzuki and Koarai, 1989**). We provide a revised understanding on the active structure distribution of the Haramachi segment and its estimation of the last earthquake event from high resolution remote sensing data, such as DEM and topographic anaglyph images.

2. Regional Tectonic Setting

Northeast Japan presently overriding the subducting Pacific Plate is characterized by a wide distribution of late Cenozoic back arc sediments which fill the Miocene extensional basin (**Taira et al., 2016**). Several contractional structures have been identified as high-angle, basement-involved faults interpreted to reflect positive basin inversion of the pre-existing Miocene extensional grabens (**Sato et al., 2002**). The locations of some Miocene faults are also structurally controlled by pre-Neogene sinistral faults (i.e. the Tanakura and Futaba faults) (**Otsuki, 1992**). These sinistral faults were reactivated in the Miocene as normal faults and dextral faults, but the Miocene strike-slip displacement was fairly small compared to the pre-Neogene displacement (Otsuki, 1975). In the south-western portion of NE Japan, sedimentation during 17-15 Ma was controlled by NW trending faults. Some of these faults were formed due to the reactivation of pre-existing faults and produced basins to the west of the Futaba Fault.

The Futaba Fault separated the Abukuma Mountain from the Cenozoic sedimentary and volcanic rocks on the Pacific side (see **Figure 1**). The Abukuma Mountain is a basement-cored highland in the Fukushima Prefecture extending 60 km east to west by 200 km north to south and representing an uplifted ridge in the forearc region of northeast Japan (**Yamamoto, 2005**). The bedrock in the Abukuma Mountain is composed mainly of the Early Cretaceous granitic rocks, remnant Paleozoic

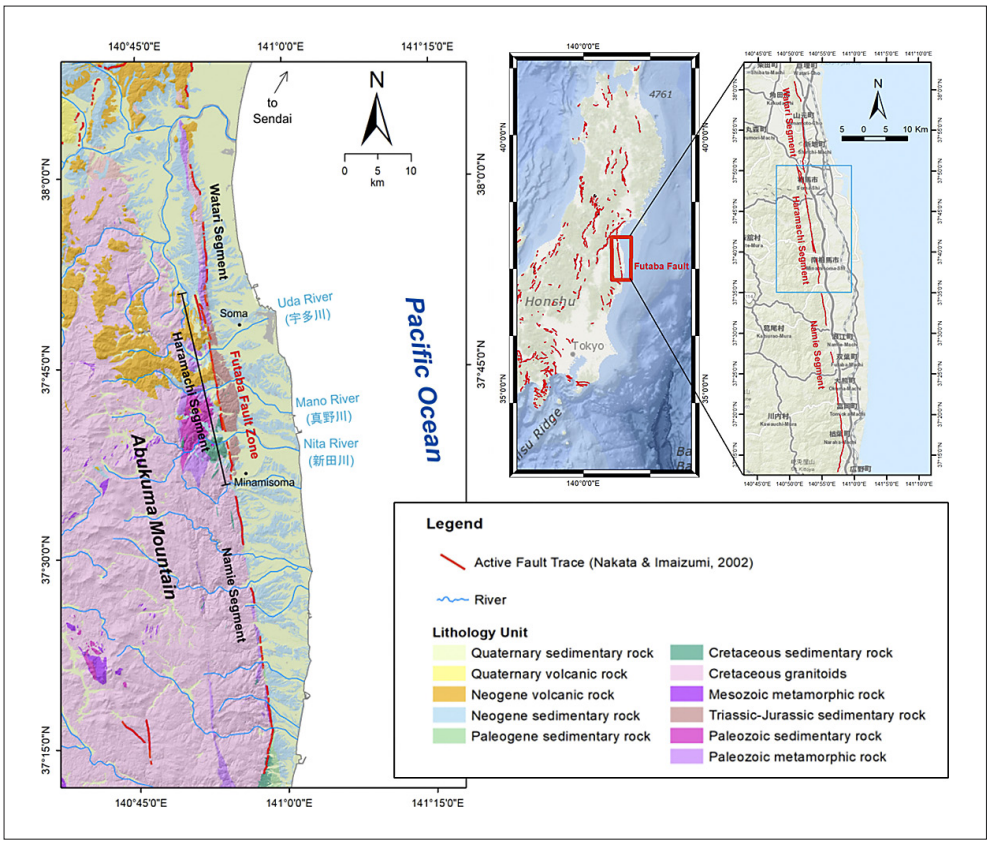

Figure 2: (left) Simplified geological map of the area of the Abukuma Mountain (modified from **Geological Survey of Japan, 2018**) showing location of active faults (after **Nakata and Imaizumi, 2002**); (middle) location of the Futaba Fault; (right) A map showing Futaba Fault segmentation and the study area (Haramachi Fault in the blue rectangle).

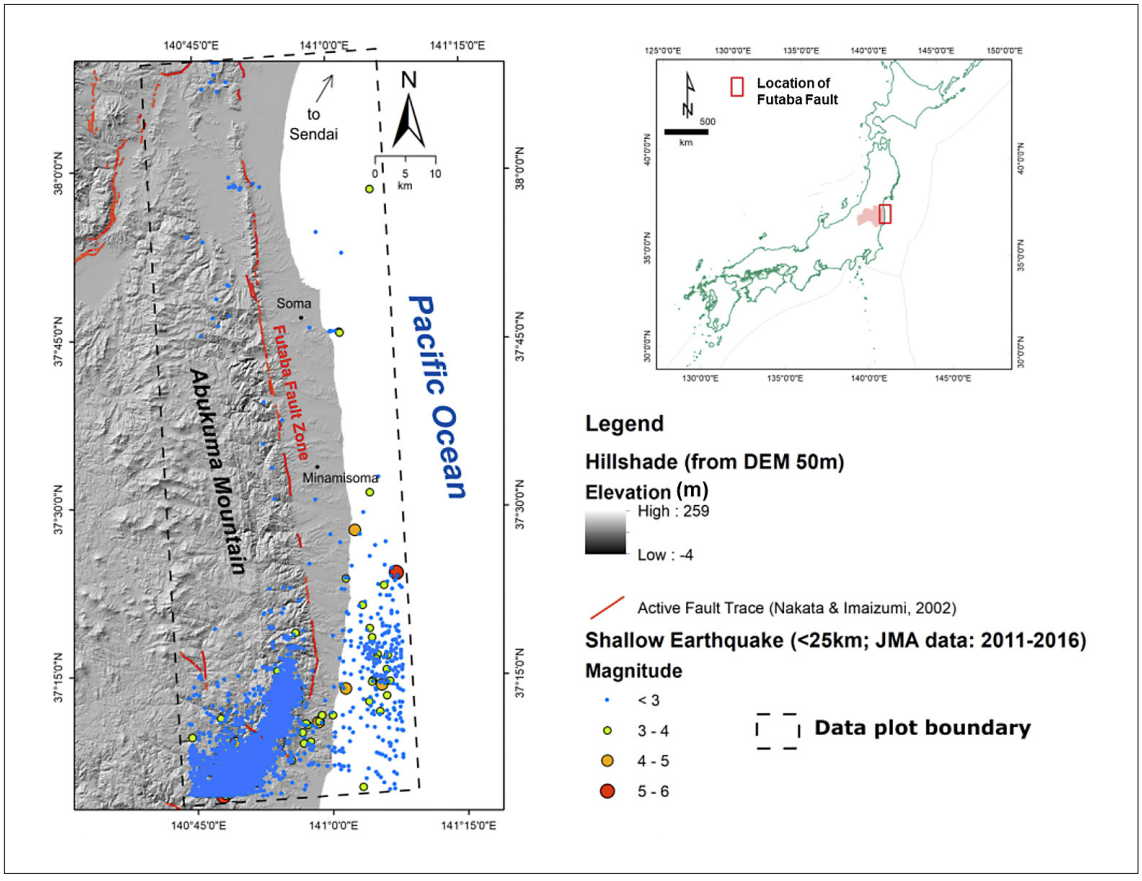

Figure 3: The swarm activity from 2011 to 2016 that occurred around the boundary of the southern Abukuma Mountain corresponding with the 2011 Tohoku Earthquake.

margin rocks, and a Middle Mesozoic subduction complex that were rifted from the Asian Mainland during Miocene back-arc extension (**Kubo et al., 2003; Regalla et al., 2010; Regalla et al., 2013**) (see **Figure 2**).

Abukuma Mountain is generally bounded on the east by N-S (N10°W) striking the Futaba Fault (**Yamamoto, 2005; Regalla et al., 2013**). The eastern side of the mountain shows clear straight boundary of the Futaba Fault. The Futaba Fault system extends for approximately 100 km along the eastern margin of the Abukuma Mountain (**Kaneda et al., 2013; Sato et al., 2013**), from northeast of Iwaki to southwest of Sendai. Futaba Fault activity has been dated back to the Late Cretaceous age (**Yanagisawa et al., 1996**). **Otsuki and Ehiro (1992)** estimated that the Futaba Fault was active in the period of 120-82 Ma and 50-40 Ma. The faulting during the first stage was associated with ductile shearing by which the crust of northeast Japan was displaced ca. 130 km. It is believed that the activity is repeated after the late Quaternary, mainly in the northern section (**Yanagisawa et al., 1996; Kaneda et al., 2013**).

Areas around the Futaba Fault had been seismically quiet before the March 2011 event, however seismicity in the southern Abukuma Mountain increased drastically following the 2011 earthquake, with several large magnitude events, up to Mw 6.1 (**Kato et al., 2011**). The extensive massive seismic swarm has continued from 2011 to present time as shown in **Figure 3**. Many of these events involved normal-sense, extensional displacements along margin-parallel planes. West-side down surface ruptures with a scarp height of up to 1.5 m were generated along the Itozawa and Yunodake faults. These events were likely triggered by static stress field changes following the subduction zone megathrust earthquake (**Toda et al., 2011**).

3. Previous Tectonic Geomorphology and Paleoseismic Studies

Previous tectonic studies have interpreted the Futaba Fault as a vertical to near-vertical fault (90°-85°W) with predominantly sinistral Quaternary slip and minor reverse displacement to the west, based on trenching of the central segment and collocation with a Cretaceous sinistral shear zone (**Fukushima-ken, 1999; Kubo et al., 2003; Regalla et al., 2010; Regalla et al., 2013**). The Futaba Fault is divided into three segments: the Watari segment, the Haramachi segment, and the Namie segment (from north to south respectively, see **Figure 2**). Quaternary ruptures are recognized only along the Haramachi segment, where Quaternary alluvium is offset, producing a 1.2 m high east facing scarp (**Fukushima-ken, 1999; Kubo et al., 2003**). The Watari and Namie segments are not categorized as active, as offset Quaternary deposits have not been observed along these segments (**AIST, 2008; Regalla et al., 2013**). However, the continuity of Watari and Namie Segment with the active Haramachi segment, and the presence of a deeply incised, steep, linear mountain front along the entire faults suggests their potential Quaternary activity (**Regalla et al., 2010**).

Matsumoto (1976) pointed out that part of the Futaba Shear Zone (FSZ) is an active seismogenic fault. **Matsumoto (1976)** noticed the existence of east-facing low fault scarp on the terrace surface at the bank of Uda River, near Soma city. He stated that there is about 15 to 100 m of sinistral displacement (ridge and river offset) with western uplift along the continuous 8 km-long trace extending from the Uda River to the Mano River. **Otsuki (1975)** also pointed out that there is a systematic sinistral bending and deflection on the river network along part of the Futaba Fault Zone (hereafter called FFZ). Signifying that the FFZ had carried out activities mainly based on vertical displacement before the Neogene-Quaternary period and has been reactivated in the Quaternary within a new stress field (dominant horizontal displacement). In the book of the "Active Fault of Japan" published by Research Group for Active Faults of Japan, a fault segment with a total length of about 70 km along the Futaba Fault trace was shown as an active fault, which was called the Futaba Fault (**RGAFJ, 1980**). About 18 km of total length, a section covering from the northern part of Soma City to Haramachi-ku in Minami-Soma City is recognized as an active fault with "Certainty 1", meaning that its existence is highly confirmed. The revised version of "Active Fault of Japan" published (**RGAFJ, 1991**) with revised data of active fault location, length, and degree of certainty, adopted the same data from the old book version. In the geological map of this area created by **Yanagisawa et al. (1996)**, the active fault trace was drawn from Soma to Haramachi-ku in Minami-Soma City, but the trace is not continuous to the more southern part.

Suzuki and Koarai (1989) found and identified the first geological record of the active fault outcrop located at Jisahara in the Kamimano River and Tochikubo in the Mano River. They classified five terrace surfaces and identified that the third terrace surface had preserved the latest fault activity record; with 1.5 m scarp height found in several points. The author assumed that the scarp was formed by the fault activity. Following their first study, they published the radiocarbon dating result of humus-rich soil layer taken in the exposed terrace surfaces along the Mano River (**Suzuki and Koarai, 1990**). They interpreted that the terrace surface is the same terrace classification as the displaced terrace surface along the Kamimano River and reported that the estimation of the radiocarbon age is 3,740 ± 120 BP, indicating that the latest movement along the fault took place less than 3,700 BP.

Fukushima-ken (1999) carried out a number of paleoseismological investigations, in the span of a three year-long (1997, 1998, 1999) investigation. Their investigation was conducted within 700 m around the Tochikubo area (along the Mano River) because the existence

of low fault scarp and fault outcrop have been reported in this area (**Suzuki and Koarai, 1989**). Benefiting from many trenching investigations and radiocarbon dating resulted in having successfully identified the age bracket of the latest fault activity (2,200-1,900 BP) and the timing of the penultimate earthquake event (12,000-9,500 BP). Thus, the authors concluded that the earthquake recurrence interval in the study area is 7,500-10,000 years. The authors also claimed to have identified sinistral offset from a detailed examination on the shape of the paleochannel at the base of trenching site. The offset was estimated to be 1.5 m, which concluded that the sinistral slip rate is 0.05-0.15 mm/year.

Corresponding to the 1995 Kobe disastrous earthquake event, Japan was in urgent need of extensive active fault study and evaluation. However, the map of the active faults that was available (**AFRG, 1991**) was not widely distributed. **Nakata and Imaizumi (2002)** reinterpreted aerial photographs and have depicted many potential active fault traces. They compiled the active fault traces on topographic maps at a scale of 1:25,000. In the "Digital Active Fault Map of Japan", the fault trace in the Futaba Fault Zone was extending about 100 km and defined as a "presumptive active fault". The area which is identified as a certain active fault extends for 13 km from Soma City to the North of Haramachi-ku in Minami-Soma.

The Headquarters for Earthquake Research Promotion (HERP) of the Ministry of Education, Culture, Sports, Science and Technology (MEXT) conducted a long-term evaluation on the Futaba Fault in 2005 (**HERP, 2005**). They defined that the section which is confirmed to be tectonically active extends about 40 km from Watari-cho in Miyagi Prefecture to Haramachi-ku at the northern end of Minami-Soma city. HERP estimated the future magnitude to be around 6.8 to 7.5. They adopted the survey results of **Fukushima-ken (1999)** which yields the estimation of the latest earthquake activity to be 2,400 to almost 2,000 cal BP; whereas the penultimate earthquake event is estimated to be 14,000-10,000 cal BP meaning that the recurrence interval lasts between 8,000 to 12,000 years; whereas slip rates are 0.05–0.15 mm/yr. The authors also set the probability of the occurrence of an earthquake within 30 years to almost 0%. However, corresponding to the 2011 Tohoku Earthquake, they determined that the Futaba Fault has emerged as one of the major active fault zones that may have a high probability of earthquake occurrence (**HERP, 2011**).

Kaneda et al. (2013) concluded that the observed active fault trace presents only a single trace (with small steps and branches in some part) extending from the Soma to the south of Minami-Soma. They called the active fault section the "Futaba Fault". The entire section (including the estimated active fault segments) including those located on the extension of the Futaba Fault or running alongside the Futaba Fault, were called "Futaba Fault Zone". **Kaneda et al. (2013)** estimated the fault length of the active part of the section to be about 32 km. This estimation was longer than the previous study due to the largely south-extended fault trace interpretation.

4. Methodology

In this study, we utilize 2m-mesh resolution DEM obtained from the Yokoyama Geo-spatial Information Laboratory. The DEM covers areas from the Shiode Mountain to the Hatsuno region in Soma City (hereafter referred to as the "northern Haramachi segment"). This DEM data was generated from the Airborne LiDAR (light detection and ranging) survey. To date, no published studies have used a similar resolution for the active fault mapping in this area. At the same time, the 5m-mesh and 10m-mesh resolution DEM from the Japan's Geospatial Information Authority (GSI) were used to map the active faults covering from the southern Shiode Mountain to Haramachi-ku at Minami-Soma City (hereafter referred to as the "southern Haramachi segment"). These datasets are the highest resolution datasets in Japan that are open for public research use and they can be obtained from the GSI website database: https://fgd.gsi.go.jp/download/menu.php.

Research methodology was based on the analysis of a slope and openness (positive and negative) topographic map obtained from Yokoyama Geo-spatial Information Laboratory, to support the recognition of geomorphic features related to active faulting, such as: deformed terrace surfaces, ridge, channel network (**Keller and Pinter, 2002; Yeats et al., 1997**) (see **Figure 4**). A slope map represents finer structures of slope variation in terrain edifices. However, slope maps computed from DEM commonly have an unsatisfactory wormlike appearance that reflects the method of contour gridding and obscures the true configuration of the land surface. **Yokoyama et al. (2002)** has introduced the "openness" term, an image-processing technique that generates an angular measure of surface form that visualize the topographic dominance or enclosure of any location on an irregular surface represented by DEM (**Prima and Yoshida, 2010**). The resulting maps of "openness" superficially resemble digital images of shaded relief or slope angle but emphasize dominant surface concavities and convexities. The values of openness require no light source, therefore relief shading limitation can be removed using this type of thematic map. Openness has two viewer perspectives, positive and negative. The positive openness map is a characteristic quantity to describe sky extent over a grid, taking large values of convex landform such as ridges. The negative openness map is a characteristic quantity to describe underground extent, taking large values of concave landforms such as river valleys. The emphasis of terrain convexity and concavity in openness maps facilitates the interpretation of landforms. **Figure 4a** shows the distinctive patterns between slope, nega-

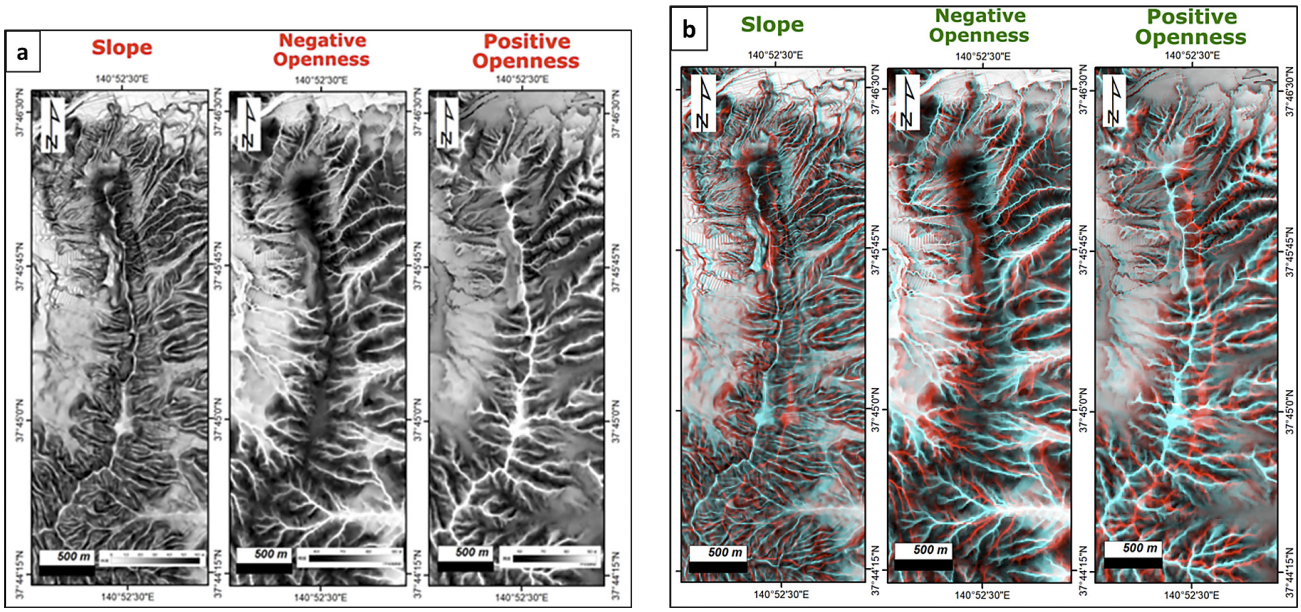

Figure 4: (a) Distinctive landform pattern shown in slope and openness maps of the Shiode Mountain area; (b) Anaglyph images of each thematic maps (slope, negative openness, and positive openness) which emphasized the systematic sinistral displacement at the eastern foot of the Shiode Mountain. This image should be viewed using red-blue glasses to provide a three-dimensional perspective.

tive openness maps, and positive openness maps. **Kanisawa et al. (2000)** has showed that using slope and openness maps derived from DEM, structural and tectonic relief can be visually identified.

Moreover, the anaglyph version of thematic maps used in this study is used to provide 3D perspective because the delineation of active faulting would still be difficult, especially if the deformation rate in a certain region is low. The anaglyph method is one of the most reliable approaches to increase the accuracy of active fault mapping. Anaglyph images are a low cost (in terms of viewing hardware), rapid method for visualizing 3D information that can be viewed in hardcopy format or on a PC screen using red-and-cyan glasses. As stated by **Hall et al. (2004)**, an anaglyph image is an established way of visualizing information in three dimensions using red-blue or red-cyan (blue-green) glasses. A terrain model is used to create an offset between a red and blue image in proportion to the elevation at a particular point. Areas of higher elevation within the image, corresponding to those points closer to the observer, will have a greater separation between the blue and red image. The left eye looking through the red lens will only see the red image with the blue image blocked, while the right eye looking through the blue/cyan lens will see only the blue image with the red image blocked. These two images are combined by the brain to produce a single 3D image, with colours other than red and blue passing through the filters . Anaglyph images can be produced from the combined detailed DEM which allows for the identification of broad tectonic deformations as well as other small changes by viewing topography exaggerated vertically (**Goto, 2016; Patria et al., 2021**). The topographic anaglyph image derived from 2m-mesh and 5-m mesh resolution DEM was used to identify the small and subtle topographic features related to active faults utilizing ArcMap and Simple DEM Viewer (available at http://www.jizoh.jp/).

We also use the combination of 1:50,000 scale geological maps published by **Yanagisawa et al. (1996)** and the Seamless Digital Geological Map of Japan (GSJ) to evaluate whether the interpreted lineaments coincide with the mapped inactive structures or lithological boundaries and to identify the fluvial terrace distribution for further terrace surface classification.

We then conducted field checking based on the DEM interpretation and conducted a borehole survey (165 cm deep) in order to assess and validate the timing of the most recent event in the Haramachi segment. The borehole survey was conducted using a portable hydraulic/percussion drilling machine to collect carbon material buried in the terrace deposit for radiocarbon dating. Finally, we measured the new estimation of Haramachi segment's total length and calculated the maximum potential magnitude of the earthquake that could be generated using the empirical relationship between surface rupture length and moment magnitude (**Wells and Coppersmith, 1994**) and Matsuda's Equation (**Matsuda, 1975**).

5. Remote-sensing and Field Observation Result

Based on the interpretation from remote sensing data, the total length of the Haramachi active fault trace is estimated to be 25 km. The fault activity can be observed from the deformed geomorphic features extending from

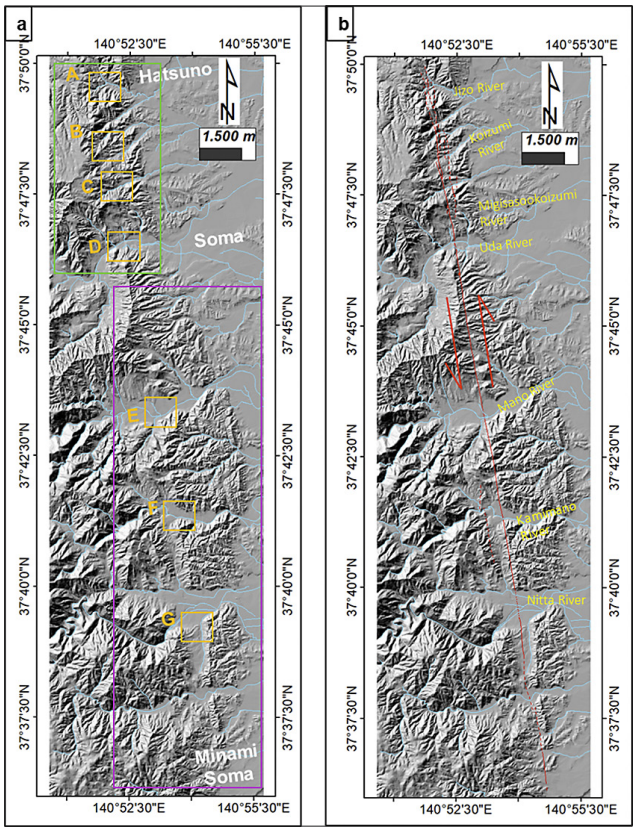

Figure 5: (a) 3D shaded relief map (10-m, from GSI) showing the observation site in an orange box (A: Hatsuno, B: Seinazawa, C: Yamagadaira, D: Yamakami, E: Tochikubo, F: Jisahara, G: Haramachiku Ogai), the blue line indicates a river, the green rectangle depicts the area of the northern Haramachi segment, and the purple rectangle shows the area of the southern Haramachi segment; (b) a 3D shaded relief map showing the interpreted fault trace of the 25 km-long Haramachi Fault.

the Hatsuno region in Soma City (northern-most part of the Haramachi segment) to near the city center of Minamisoma (the southern-most part of the Haramachi segment) in Fukushima Prefecture (see **Figure 5**). The fault trace extends almost linearly striking relatively N10°W with many sinistral fault movement indications.

In the study area, terrace deposits are present at multiple levels along the main rivers in the hilly and mountainous areas. There are four main rivers flowing from the west to east Abukuma Mountain into the Pacific Ocean and are responsible for the incision of the well-developed Pleistocene to Holocene terrace. From north to south, they are named: Uda River, Mano River, Kamimano River, and Nita River. At the mountainous region in Hatsuno, the fault was observed to cross several small rivers, namely: Migisasookoizumi River, Koizumi River, and Jizo River (see **Figure 5**).

On the basis of surface continuity and the degree of surface incision clarified from the DEM and topographic anaglyph image interpretation, the terrace surfaces are classified into higher (H), middle (M), lower (L1, L2, L3) and alluvial deposit (Al) in descending order. These classifications are slightly different from previous studies (**Suzuki and Koarai, 1989; Yanagisawa et al, 1996; Kaneda et al, 2013**) that used surfaces divided based on height difference of the terraces. The revised classification is constructed because several younger strath terraces can be observed from the high-resolution material used in this study. The lowest terrace surface is the most important geomorphic marker for identifying the timing of the most recent earthquake event.

The field investigation was done repeatedly to refine the identification of fault traces and to correlate the terrace surface classification. Fault outcrops found in the field provide evidence of both faulting and displacement. The fault mostly juxtaposes two different lithologies of different age. On the west side/wall of the fault trace was dominantly bounded with the Nakanosawa Formation (consists of sandstone, limestone, and shale) deposited in the Cretaceous, whereas on the eastern side/wall of the fault, it is mostly composed of Early Miocene Shiode Formation (consists of sandstone and conglomerate).

5.1. Northern Haramachi Segment

The area from the northern Shiode Mountain (Yamakami) to the Hatsuno region in Soma City is referred to as the northern Haramachi segment (see **Figure 5**). The geomorphic features which could be a clue for recent faulting along this part of the segment was observed from aspects of offset terrace surfaces, fault scarps, deformed pressure ridges, saddle, and displacement of river network. Many subtle lineaments were observed parallel with the main trace and as branching faults from the main fault trace. The river terraces are well-distributed only along the Uda River. The region situated at the north side of Uda River is characterized by hills or mountains, causing the lower terrace surface to decrease in altitude towards the southern end of the northern Haramachi segment.

5.1.1. Hatsuno Site

In the upstream region of the Jizo River, the young terrace surfaces are poorly distributed. It is estimated to be dominantly deposited by L1 surface along the upstream side (see **Figure 6a**). This is consistent with the classification of Yanagisawa et al. (1996). A small scarp can be observed near the curvy road of Route 228, which is estimated to displace the L1 surface vertically (C-C' profile). A linear valley can also be observed along the tributary channel of the Jizo River. However, the trend of both the estimated fault scarp and linear valley bends more westwardly compared to the scarp trend observed south from this site. The changing of orientation of these features suggests that the fault segment termination is approaching this location.

At this site, an outcrop exposing a ca. 2-3 m wide fault shear zone including a series of black fault gouge in the terrace base along the upstream side of the Jizo River

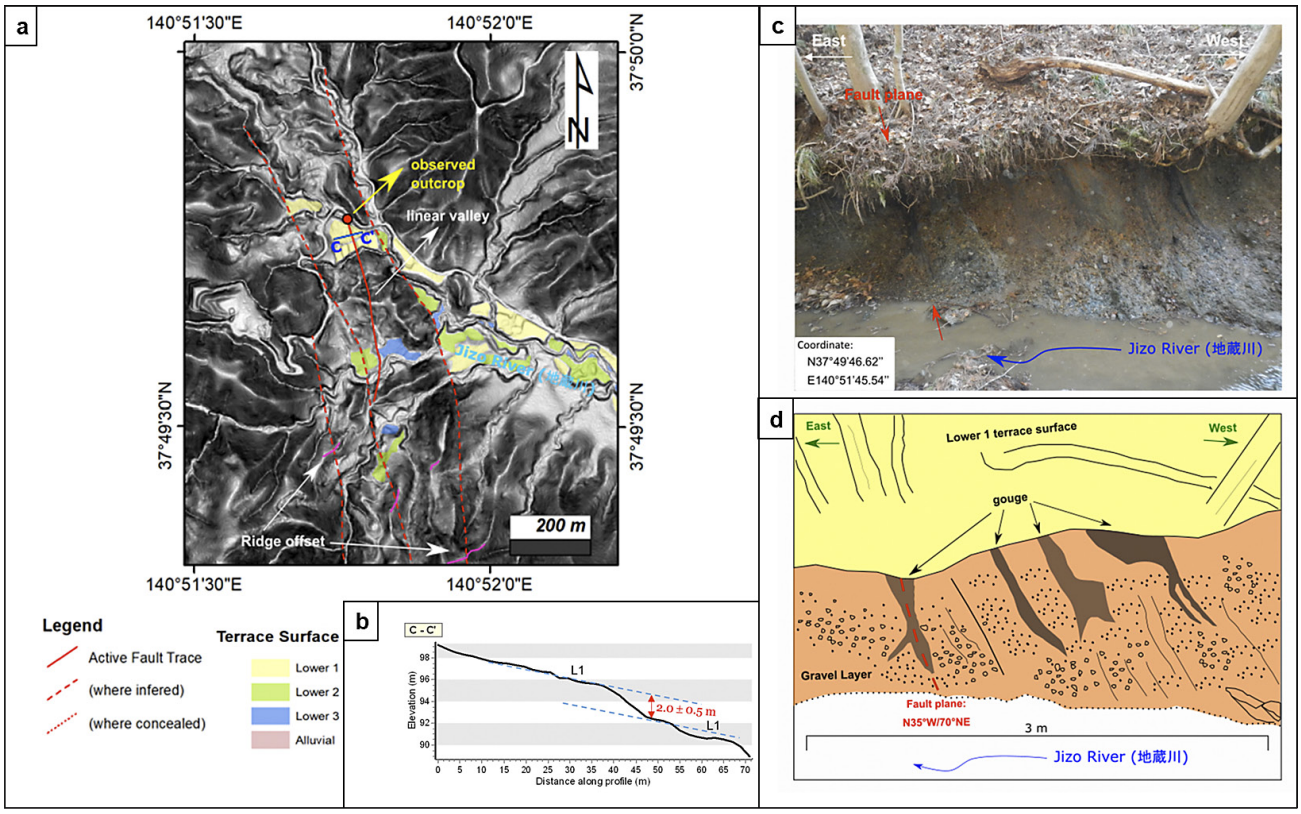

Figure 6: (a) The distribution of terrace surfaces and active fault trace along the Jizo River overlaid on a 2-m slope map; (b) Topographic profile C – C' across the fault trace; (c) Fault outcrop photograph; (d) Corresponding annotated sketch of the fault outcrop observed in the upstream side of the Jizo River.

is observed (see **Figure 6c**). The spatial distribution of young terrace surface is very poor in the upstream region of the Jizo River. The estimated scarp observed from the remote sensing data could not be located clearly in the field. Although this area does not preserve clear evidence of deformation compared to its southern segment, the series of soft clay fault gouge found in the field are taken as a signal indicating that the active fault deformation has reached into this region.

5.1.2. Seinazawa Site

Linear valley features can be observed continuously in a NNW-SSE trend until it reaches the Seinazawa region near the upstream side of the Koizumi River (see **Figure 7a**). From this region, several parallel fault strands can be delineated based on the saddle observed on the deformed pressure ridge. The deposit of terrace surface is rather difficult to distinguish in this site due to poor development. It is estimated that the lower 3 (three) river terrace still exists in this site, although **Kaneda et al. (2013)** classified the terrain at this site as alluvial lowland.

A large fault outcrop is exposed right on the side of the curvy road leading to Seinazawa (see **Figure 7b**). At this outcrop, a 3 m wide fault shear zone was recognized. The fault plane strike and dip are N20°W and 59°NE, respectively. The fault appears to be a normal fault. The greyish black soft fault gouge (consists of clay and silt) is bordering two different lithologies: the fractured greyish limestone bedrock (Nakanosawa Formation, Cretaceous) on the west and a weathered brownish-cream-colored sandstone (Shiode Formation, Miocene) on the eastern side of the fault. On top of the exposure, about 30 cm thick of soil interval overlays the bedrock. There is no clear indication of faulting in the soil layer at the top.

5.1.3. Yamagadaira Site

The linear valley is elongated until it reaches the Yamagadaira site along the Migisasookoizumi River. Here, the lower terrace surface can be observed due to good preservation. However, according to **Kaneda et al. (2013)**, the terrain in this region is classified as alluvial lowland. Approximately 300 m eastward from the main fault trace, small fault scarps could be detected from 2m DEM and topographic anaglyph image (see **Figure 8a**). The topographic profile B – B' shows a subtle scarp with about 1.5 m vertical displacement on the estimated L3 surface. Thus, the presence of a parallel fault strand can be indicated by the emergence of this feature. **Kaneda et al. (2013)** identified the same scarp but they classified them as presumed active faults.

In the field, the subtle scarps trending N10°E can be recognized on the terrace surface exhibiting horizontal displacement of about 8 m. Additionally, about 80 m

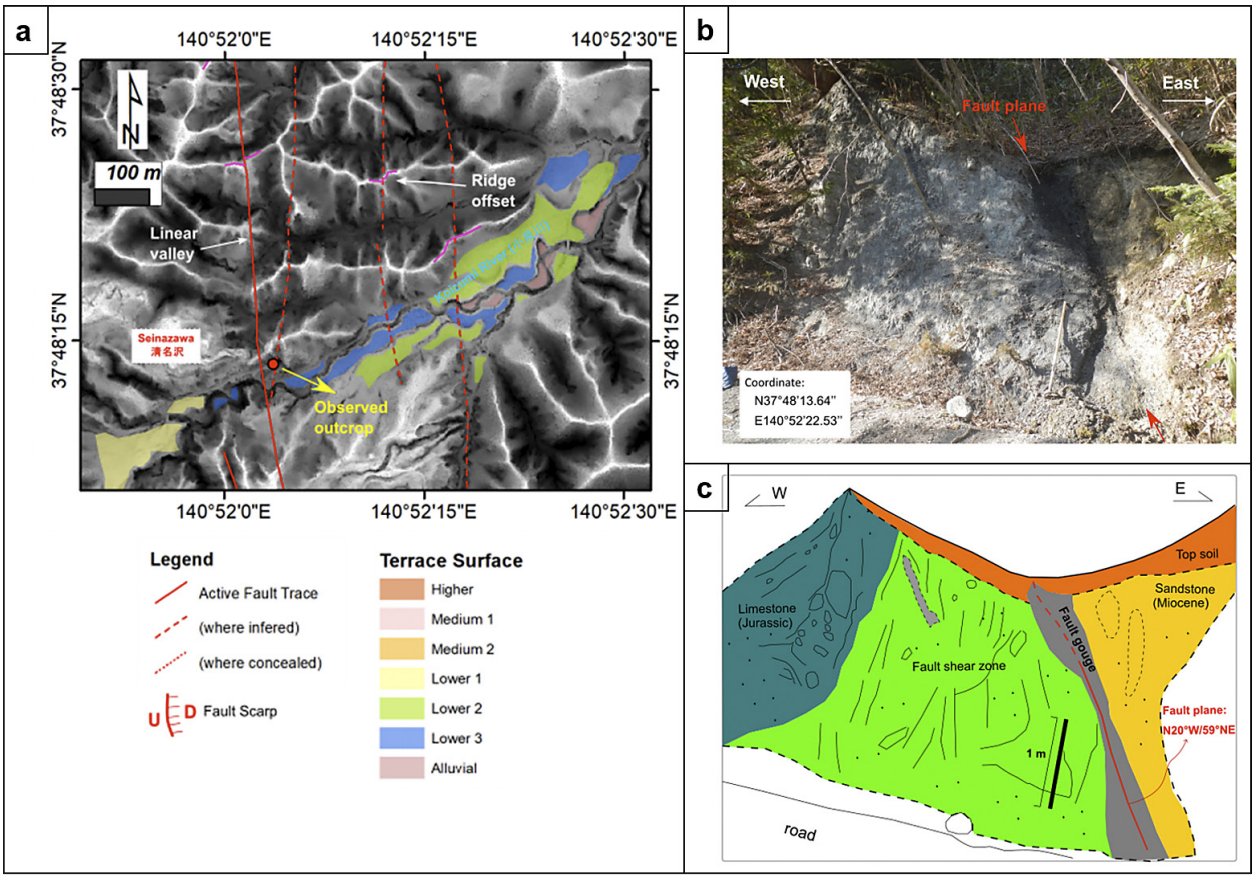

Figure 7: (a) The distribution of terrace surfaces and active fault trace along the Koizumi River near the Seinazawa site overlaid on a 2-m positive openness map; (b) Fault outcrop photograph; (c) Corresponding annotated sketch of the fault outcrop observed on the road side leading to Seinazawa, near the Koizumi River.

northward from the identified scarp, the riverbed seems to be deflected to the east (see **Figure 8c** & **8d**). The trend of the estimated scarp in the river is consistent to be around N10°E. Thus, the field evidence of these features confirmed the presence of an active deformation.

5.1.4. Yamakami Site

There are five terrace surfaces along the Uda River identified in Yamakami site located near the Shiode Mountain, named: M2, L1, L2, L3, and Al in descending order. The M2 surface is mostly distributed at the foot of the Shiode Mountain in a fan-shape. It was probably deposited from the tributaries of the mountain. The L1 surface is well-preserved in this region and distributed widely along this river. The L2 surface formed below the L1 surface as a strath surface. The L3 surface is the lowest terrace surface observed at this site.

A prominent scarp displacing multiple levels of terrace surface is observed through DEM and topographic anaglyph images (see **Figure 9a**). The scarp has a NNW-SSE trend and displaces all of the lower terrace (L1, L2, L3) at this site. The topographic profile shows a vertical displacement of about 2.5 m (west-side-up) in the L3 terrace surface. The disrupted sediment underlying the scarp may indicate that the scarp is likely associated with the latest active faulting event that ruptured after the abandonment of the L3 terrace surface. In addition, the scarp aligns consistently with the clearly defined linear topographic break (saddle) that can be seen at the eastern base of the Shiode Mountain, which causes a systematic bend and displacement of the river network (see **Figure 10**). All directions of the river bending indicate sinistral displacement, with an amount of 100-200 m. The river displacement pattern can be observed continuously southward until it reaches the terrace surface distributed along the Mano River.

This site is preserving the most prominent fault scarp that is probably recognized by **Matsumoto (1976)** and observed by **Yanagisawa et al. (1996)** and **Kaneda et al. (2013)**. The scarp has vertically displaced multiple levels of lower terrace surface classified in this study (L1, L2, L3) with an offset amount ranging from 1.5 m to 14 m. However, the amount of this offset might not reflect natural conditions as it might be affected by the artificially made paddy field terrain. No horizontal displacement can be observed in this region.

5.2. Southern Haramachi Segment

The area from the southern Shiode Mountain to Haramachi-ku in Minami-Soma City is referred to as the

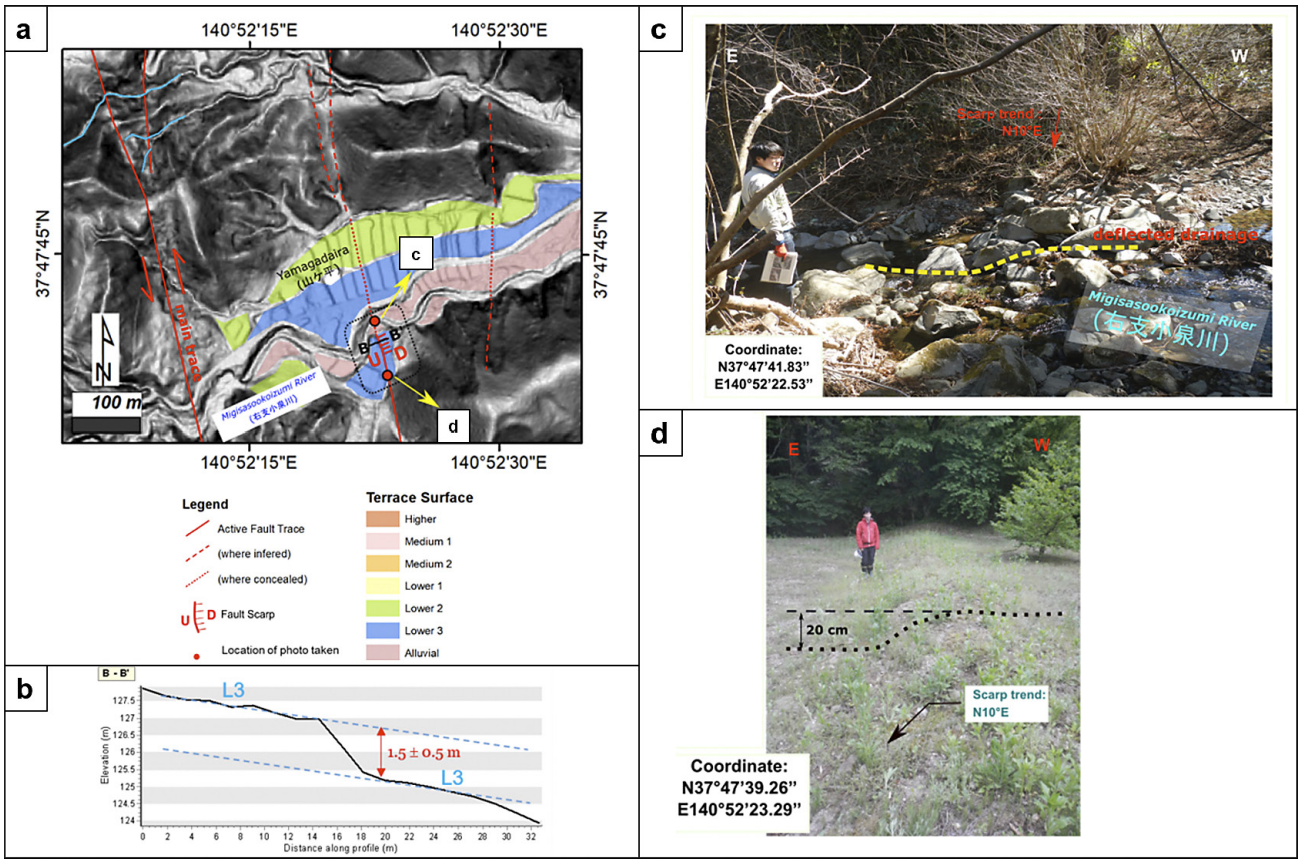

Figure 8: (a) The distribution of terrace surfaces and active fault trace along the Migisasookoizumi River in Yamagadaira site overlaid on 2-m slope map; (b) Topographic profile B – B' across the fault trace; (c) Deflected drainage river bed; (d) Subtle fault scarp in L3 terrace.

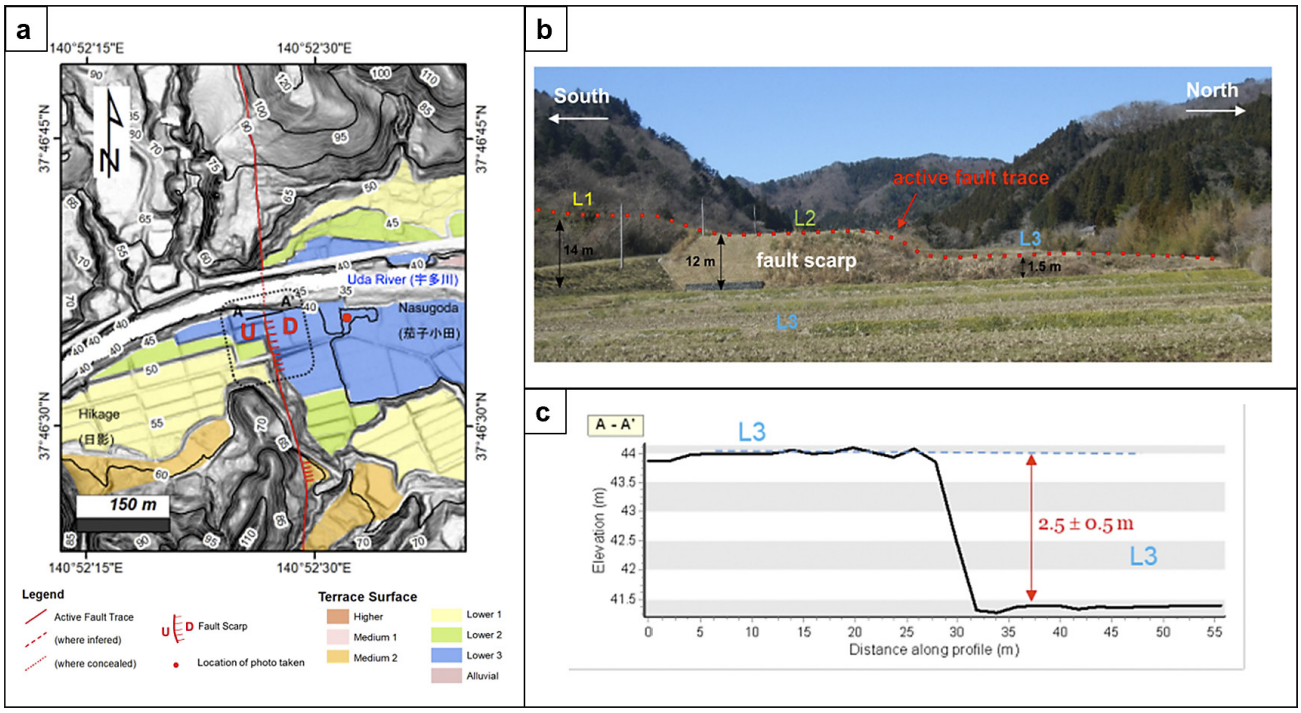

Figure 9: (a) The distribution of terrace surfaces and active fault trace along the Uda River in the Yamakami site overlaid on 2-m slope map, showing a 5-m contour interval; (b) Photograph of fault scarp at the Yamakami site along the Uda River; (c) Topographic profile A – A' across the fault trace.

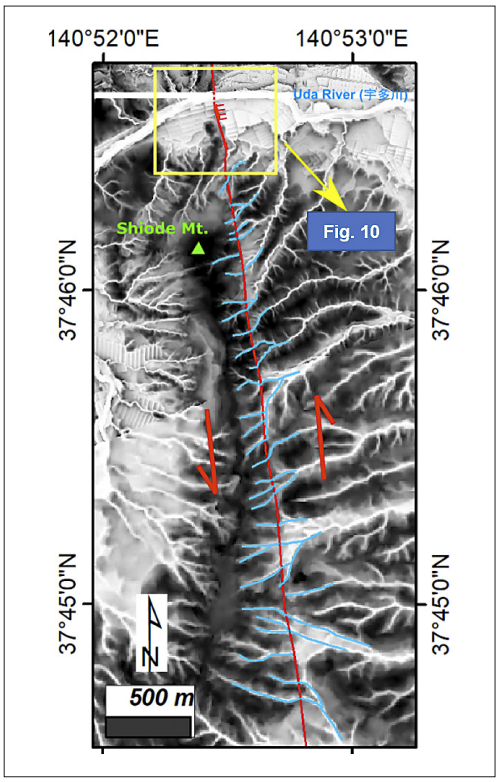

Figure 10: Systematic sinistral offsets and deflections of the river at the eastern foot of the Shiode Mountain overlaid on a 5-m negative openness map.

southern Haramachi segment. This region is located in a relatively low elevation compared to the northern Haramachi segment area. The terrace surface is well-developed along the main river in this part of the segment (the Mano River, the Kamimano River, and the Nita River). Thus, geomorphic features which indicate active faulting can be observed based on scarp on the terrace surface and the river offset which incised the displaced terrace surface. A few of the parallel fault strands can be noticed as well and delineated in the Jisahara region. The active fault trace in southern part of the segment is estimated to stop at Yakushimae close to the Yokokawa Dam in Minamisoma, due to the absence of a lower terrace surface which is displaced by the fault.

5.2.1. Tochikubo Site

The fault trace in this region (Tochikubo) can be continuously delineated southward based on the linear saddle on the eastern foot of the Shiode Mountain. In the Tochikubo region, the lower 3 terrace surfaces are well-developed alongside with more broad distribution of alluvial deposits to the downstream area along the Mano River. Several scarps are observed on the lower 3 terrace surfaces from the topographic profile generated from the 10-m DEM of GSI, which yields a vertical displacement of 1.5-2.5 m (see **Figure 11a**). The fault trace is continuous to the southern region.

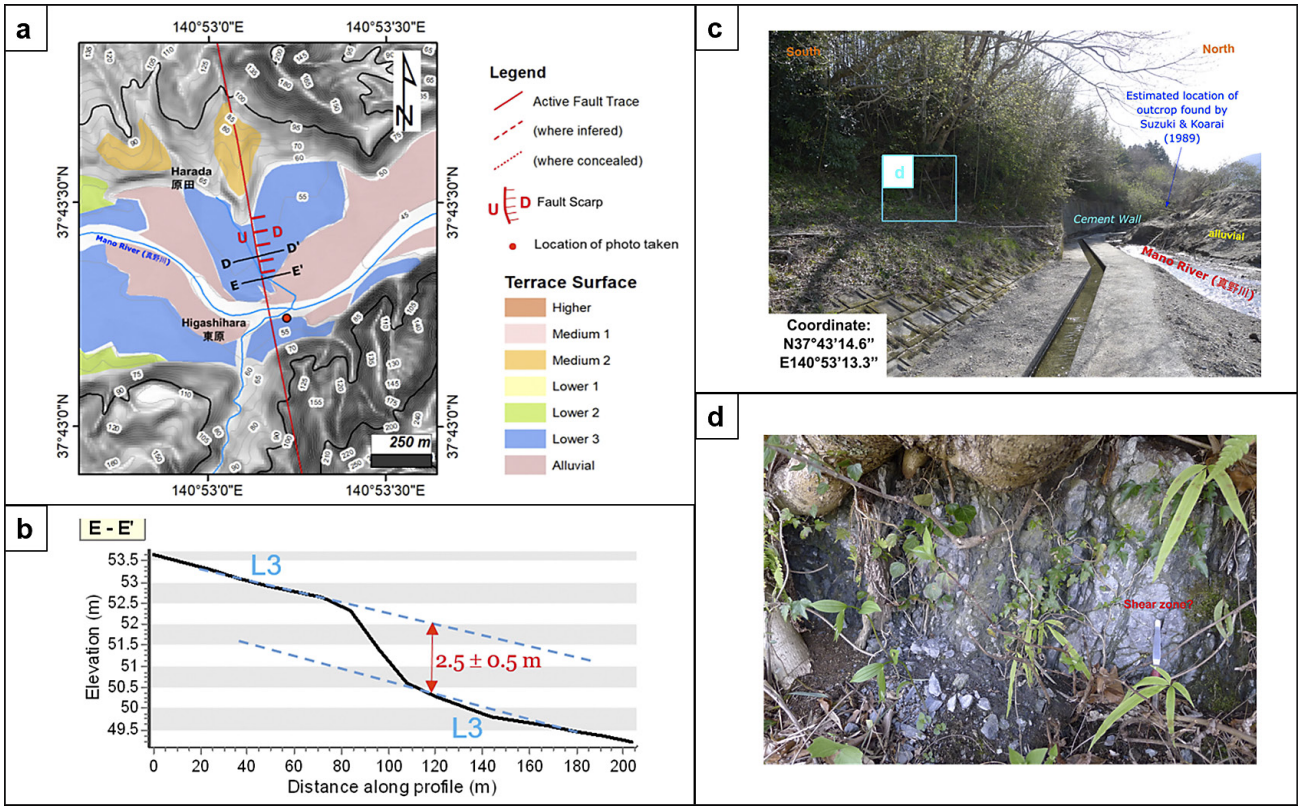

Figure 11: (a) The distribution of terrace surfaces and active fault trace along the Mano River overlaid on a 5-m slope map with a 5-m contour interval; (b) Topographic profile E – E' across the fault; (c) The estimated observation location of **Suzuki and Koarai (1989)**; (d) Shear zone outcrop observed at the southern bank of the Mano River.

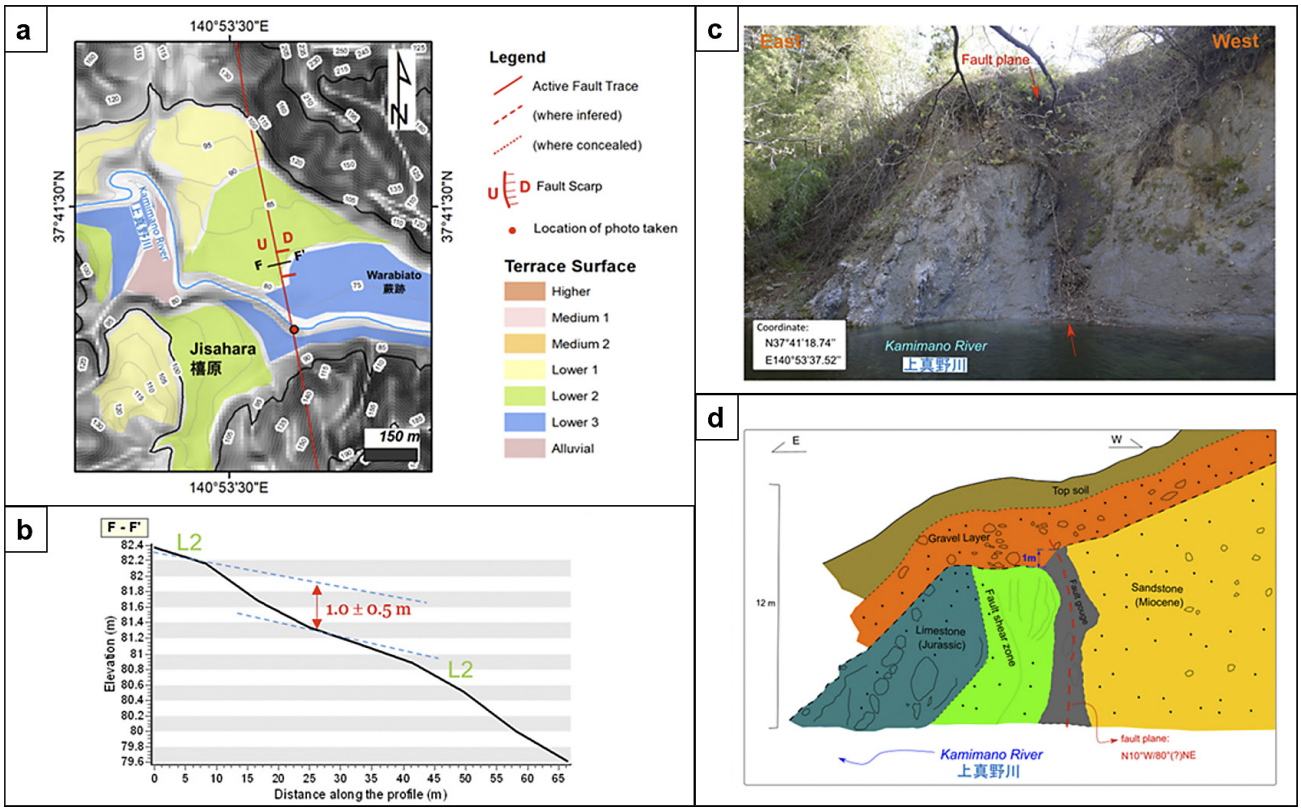

Figure 12: (a) The distribution of terrace surfaces and active fault trace along the Kamimano River overlaid on a 5-m slope map with a 5-m contour interval; (b) Topographic profile F – F' across the fault trace; (c) Fault outcrop photograph; (d) Corresponding annotated sketch of the fault outcrop observed in the Jisahara site.

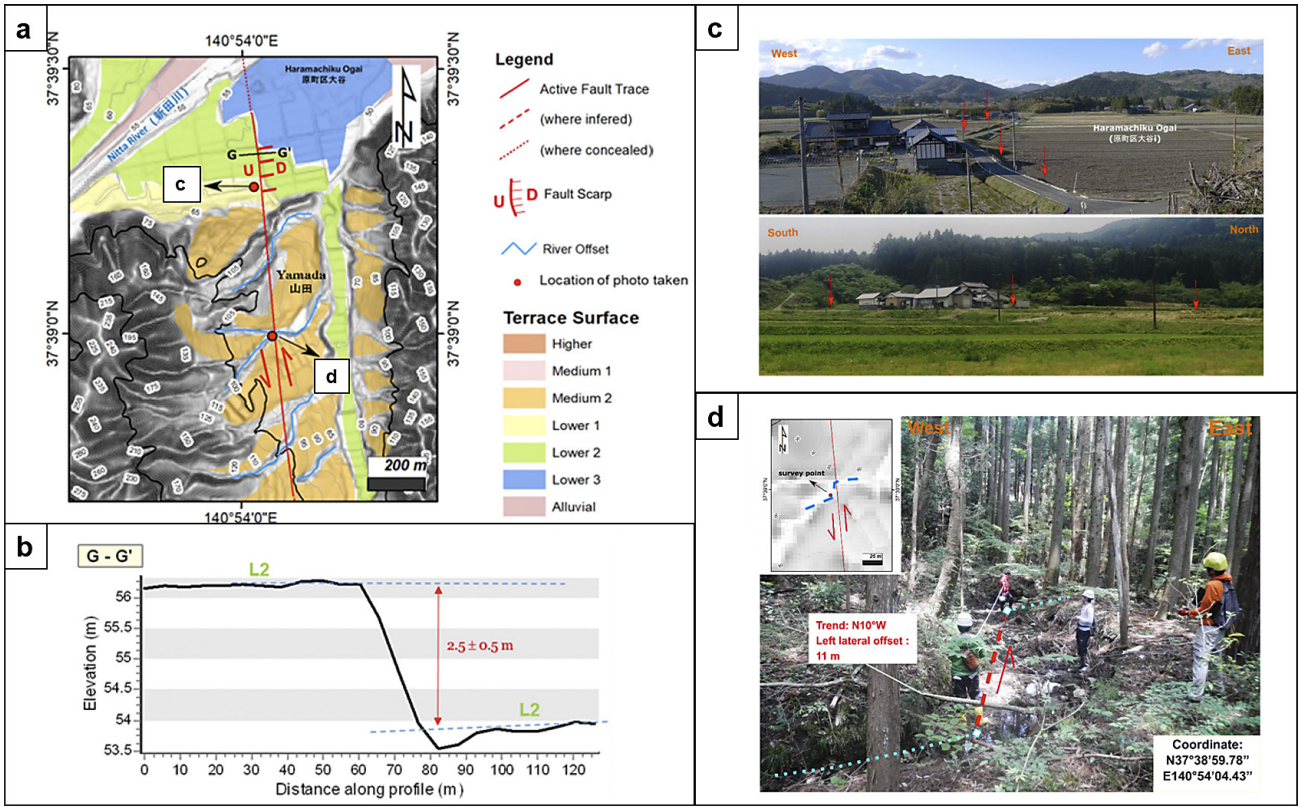

Figure 13: (a) The distribution of terrace surfaces and active fault trace along the Nita River overlaid on a 5-m slope map with a 5-m contour interval; (b) Topographic profile G – G' across the fault trace; (c) Low fault scarp observed along the Haramachiku Ogai paddy field; (d) About 11 m left lateral offset channel observed in the Haramachi-ku Ogai site.

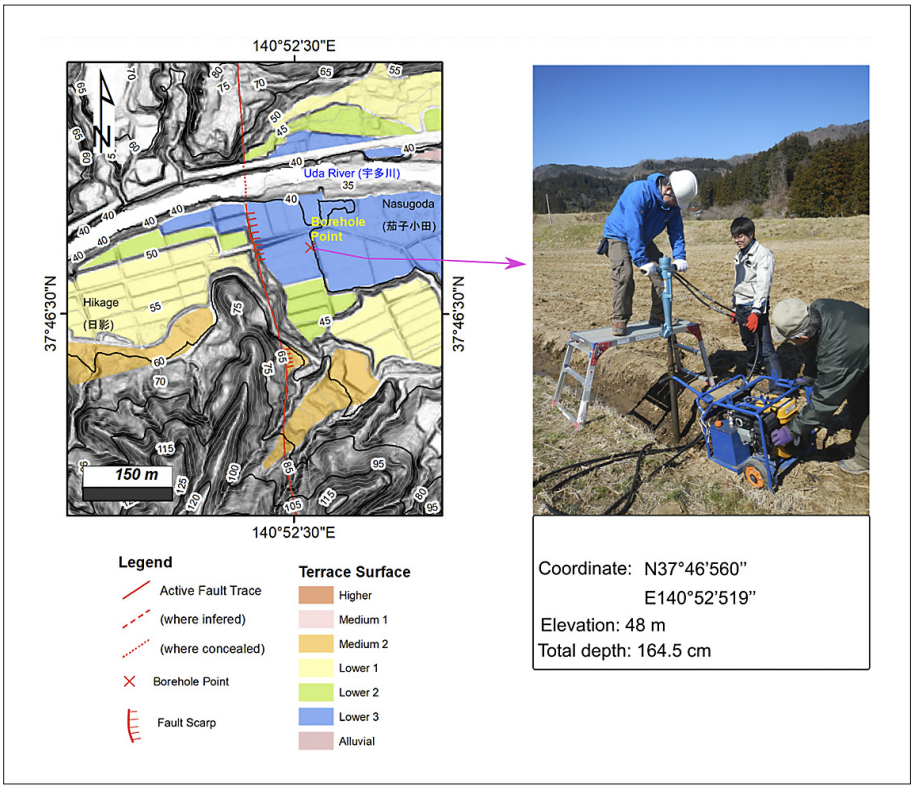

Figure 14: (left) Map showing the borehole survey point (x mark); (right) Borehole execution on the L3 terrace by the Uda River.

In the Tochikubo region along the Mano River, an estimated shear zone exposure was observed. **Suzuki and Koarai (1989)** found a fault outcrop at this site. Unfortunately, the outcrop is now covered by a high cement wall (see **Figure 11c**). The outcrop observed in this study has a small dimension, which is only about 1 m x 80 cm classified as a lower 3 terrace. The bedrock is highly fractured and intercalated with grey clay gouge. The small shear zone can be inferred from the outcrop which shows vertical crushed material related to recent faulting (see **Figure 11d**). Therefore, this particular outcrop serves as a marker for outlining the continuous path of the active fault trace, supported by many trenches of **Fukushima-ken (1999)**.

5.2.2. Jisahara Site

The consistent NW-trending fault can be followed from the south of the Mano River to the left bank of the Kamimano River in Jisahara (see **Figure 12a**). The lower terrace surface in Jisahara is well-distributed. A subtle fault scarp is revealed by the topographic map derived from 10-m GSI DEM, which vertically displaced the terrace between the lower 2 terrace surface and the lower 3 terrace surface. The amount of vertical displacement is about 1 m, with the east side down as observed at the other site. **Suzuki and Koarai (1989)** observed the displacement on the right side of the Kamimano River, which becomes the marker to continuously delineate the fault trace southward. A parallel lineament was observed from the linear topographic break in the Jisahara region across the main fault trace. However, no reliable displacement is observed, thus the trace is classified as an inferred fault trace. In the map of **Kaneda et al. (2013)**, an estimated fault trace is also observed in this region. However, their interpretation displays it as a rather curvy line.

The fault outcrop shown in **Figure 12c** found at the right bank of the Kamimano River in Jisahara has been described in many studies (**Suzuki and Koarai, 1989; Kaneda et al., 2013**). At this site, the fault plane juxtaposes the fractured limestone (*Nakanosawa Formation*) to the eastern side with sandstone (Shiode Formation) to the western side. A sub-rounded gravel layer overlays the bedrock. About 1 m of vertical separation at the bottom of gravel layer is recognized. Brownish top soil was deposited on top of the gravel layer. Greyish-black soft fault gouge with a width of about 5 cm is present in the middle part of the fault plane. However, the outer margin of the gouge (about 50 cm wide) was rather consolidated. The strike and dip of the fault plane is estimated to be N10°W and 80°NE. The shear zone of the fault is estimated as 3 m wide. The degree the fractured zone of the bedrock is getting more intense reaching to the center part of the fault plane area. No offset can be observed on top of the terrace deposit.

5.2.3. Haramachiku Ogai Site

Southward from the Jisahara site, a systematic left-lateral deflection of the river with an amount ranging from 50 to 200 m displacement can be observed near the hilly area of Yanagidaira. That feature becomes the marker to delineate the fault trace. However, the fault

trace seems to be concealed under the paddy field in the left bank of the Nita River. A fault scarp can be identified again of the right bank of the Nita River (Haramachiku Ogai paddy field), displacing the lower terrace surface by about 2.5 meters vertically. Also, streams incised into the M2 surface exhibit around 7-12 m left lateral offset near Yamada (see **Figure 13a**).

In this region, no active fault exposures are observed in field along the estimated fault trace. However, a low fault scarp of about 1 m high can be recognized. The scarp coincides with the small road along the paddy field in the southern bank of the Nita River at Haramachiku Ogai (see **Figure 13c**; red arrow shows the trace of the scarp). The scarp trend is consistent with the trend observed from the remote sensing data (N10°W). Following further south, in the forest area near Yamada, a small channel was recognized to have a left bending or offset of about 11 meters (see **Figure 13d**).

6. Borehole Survey and Radiocarbon Dating Result

In order to assess and validate the timing of the most recent event in the Haramachi segment, we conducted a shallow drilling project, a usable borehole survey using portable and collected carbon material buried in the terrace deposit for radiocarbon dating.

The best selected site is in the paddy field at the Yamakami site along the Uda River (see **Figure 14**). There is a clear vertical offset of the lowest terrace surface, with the western part being the fault's hanging wall and the eastern part being the foot wall. The execution of the borehole survey decided to be on the foot wall side of the displaced terrace surface. The drilling machine successfully extracted soil sample from the terrace deposit and a full core was obtained until a depth of 164.5 cm with a consolidated gravel deposit at the bottom.

The obtained core shows 6 different sedimentation phases (see **Figure 15**), which from top to bottom are described as follows:

1. Cultivated soil (top to -50 cm): A blackish brown sandy silt layer gradually changes colour to grey. Interpreted as artificial deposit of the paddy field soil at the present time.
2. Clay (-50 to -65 cm): This layer contains a dominantly dark grey coloured clay deposit, might be the bottom part of the artificial paddy field soil.

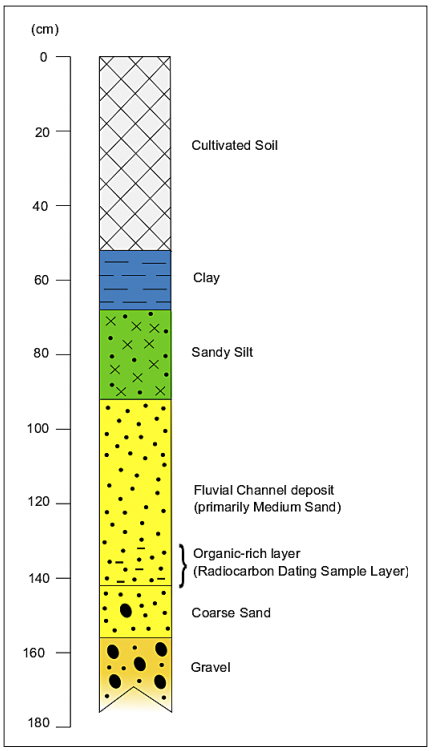

Figure 15: Stratigraphic column interpreted from the borehole core.

3. Sandy silt (-65 to -86.5 cm): This layer shows a deposition of grey sandy silt, is interpreted as the original terrace deposition. Abundant pieces of mica mineral are present in the well sorted layer.
4. Medium sand - sandy silt (-86.5 to -135 cm): This layer contains a brownish-coloured massive sand deposit. Mica mineral of weathered granitic and volcanic clasts are abundant. Based on **Yamamoto (2005)**, the typical brown-coloured massive sand deposit is known as 'flood loam' in Japan. In this layer, a range of soil organic material from depth 126.5 to 136.5 cm (sample name: FTB-1) is collected for further radiocarbon dating.
5. Coarse sand (-135 to - 156.5 cm): The colour is gradually changing to a greyish black sand layer and the grain is slightly coarser than the upper layer. Several gravels are contained in this layer. In this layer, a range of soil organic material from depth 136.5 to 146.5 cm (sample name: FTB-2) is collected for further radiocarbon dating.

Table 1: Radiocarbon dating result ($\delta^{13}C$ corrected value and calibration age).

Sample Name	Core Depth (cm)	$\delta^{13}C$ (‰)	$\delta^{13}C$ Corrected Value		1σ cal. year range (cal BP)	2σ cal. year range (cal BP)
			Libby Age (BP)	pMC (%)		
FTB-1	126.5-136.5	-24.88 ± 0.39	4,150 ± 30	59.67 ± 0.19	4814 – 4784 (15.1%) 4755 – 4754 (5.6%) 4710 – 4616 (47.5%)	4823 – 4780 (18.5%) 4770 – 4580 (76.9%)
FTB-2	136.5-146.5	-22.78 ± 0.31	3,690 ± 20	63.14 ± 0.20	4082 – 4029 (44.6%) 4011 – 3985 (23.6%)	4142 – 4128 (2.6%) 4093 – 3970 (91.5%) 3941 – 3933 (1.3%)

6. Gravel - very coarse sand (-156.5 to -164.5 cm): Dark grey unconsolidated coarse sand and consolidated gravel layer is identified of the bottom of the core. The length of a major axis of the gravel are 2 to 15 mm, primarily sub-rounded granite gravel.

The sedimentation phase analysis suggests that the typical fluvial channel deposit is observed on the lower layer of the soil strata extracted from the core, which is primarily composed of sand and gravel. It suggests that the old channel of the Uda River has passed through the borehole point. The river is expected to have meandered and changed in the natural environment like at the present time. After a certain time, the water level is interpreted to have risen and deposited the silt and clay layer on top of the sand deposit (flood plain deposit). There is no plant root observed in the whole core, meaning that the sedimentary environment was not expected to be a marsh, but rather represented a high river flow velocity.

The age of the terrace deposit can be estimated from radiocarbon (^{14}C) dating. The borehole core obtained from the field investigation did not provide a sufficient amount of carbon material in the suspected and targeted layer. Thus, bulk soil sediment was decided to be used for radiocarbon dating.

There were two bags of bulk soil sample collected from different depth ranges (labelled FTB-1 and FTB-2) that were sent to the Institute of Accelerator Analysis Ltd. (IAAA) at Fukushima prefecture. The method that was applied is Accelerator Mass Spectrometry (AMS) technique. The samples were pre-treated with acid (HCl) washes. The result is shown in **Table 1**.

The age result seems to be reversed in stratigraphic basis because technically FTB-2 should have an older age as it is taken from deeper soil sediment, however the shallower depth dating sample (FTB-1) seems to have a high risk of contamination from artificial activity. Therefore, the age result from sample FTB-2 is more reliable to be referred to as the age of the displaced terrace surface. Additionally, IAAA confirmed that the carbon content found in the measured dating sample has a low value (0.74%).

7. Discussion

Using the new approach of remote sensing and field observation data, we have confirmed that the Haramachi segment of the Futaba Fault zone is an active fault with the evidence of the vertically disrupted Holocene terrace surfaces. Our result is consistent with the investigation result of **Fukushima-ken (1999)** and **Kubo et al. (2003)**. However, the sense of slip of the fault movement is rather difficult to determine from the surface observation and limited subsurface observation in this study. The evidence can be inferred from systematic sinistral offsets and the bending of streams and ridges along the fault segment. However, there is no clear horizontal displacement found in the Holocene terrace surfaces that might be a clue of very slow slip rate. The most pronounced sinistral offset features are observed from the systematic river network offset and bending at the eastern foot of the Shiode Mountain bedrock, indicating that the displacement has resulted from a single or multiple faulting events. The linear geometry characteristic of the fault trace supports the statement that the Haramachi segment is a strike-slip fault, which is further supported by the existence of subparallel faults. Dip-slip faults usually form sinuous or irregular ridge/scarp at the surface, which is clearly different from the surface geometry of the Haramachi segment.

At the northern part of the Haramachi segment, which is mostly composed of bedrock with thin Quaternary deposits, geomorphic features associated with fractured rock was observed, such as aligned notches, saddles, and linear valleys within the bedrock. This can indicate the presence of a fault, yet only observing these geomorphic features is insufficient to determine whether or not the fault is still active. The deformation pattern of the northern Haramachi segment displays Horsetail Splay structure, which commonly occurs in strike-slip faulted marking the termination of a strike-slip fault zone. The fault displacement seems to be distributed right stepping through several splay faults from the known sinistral strike slip of the main fault plane. This would suggest that transpression deformation style is dominant in this region. In other words, the strike-slip setting in this region is experiencing restraining or contractional stepovers, or a contractional linking damage zone (Kim et al., 2004). This type of deformation is produced where the sense of step is opposite to the sense of the overall slip (e.g. a right-step along a sinistral fault or vice versa) (**Cunningham and Mann, 2007; Mann, 2007; Peacock et al., 2016**).

In this study, the recent fault activity was assessed from the evidence of the deformation of the lowest terrace surface at the northern part of the Haramachi segment (at the Yamakami site along the Uda River), because no known study has identified the timing of the most recent event in this part of the segment. This terrace surface has been dated using ^{14}C age estimation yielding 4,093-3,970 cal BP. This estimate is consistent with the ^{14}C result of **Suzuki and Koarai (1990)**. Their ^{14}C result was yielding 3,740 ± 120 BP by dating the humus-rich soil layer obtained from the outcrop at the bank of the Mano River which is located at the central part of the Haramachi segment. The consistency of radiocarbon dating result between this study and **Suzuki and Koarai (1990)** gives us a suggestion to consider that the central and northern parts of the Haramachi segment might have ruptured together in the same most recent earthquake event (based on the younger limit of our ^{14}C sample, which is around 4,093-3,970 cal BP).

Although the organic soil used for dating shows a consistency with the previous study (**Suzuki and Koarai, 1990; Fukushima-ken, 1999**), the uncertainty is relatively high due to low carbon content from both

samples (only 0.74% which is supposed to be at least 1%). Also, as stated in **Walker (2005)**, the dynamic nature of the soil system means that they receive organic matter over a protracted time period, any radiocarbon date on a soil will largely be a measure of the mean residence time of the various organic fractions within the soil. Because of the continuous input of the organic material into soils, measured radiocarbon ages of soil organic matter or its fractions are generally younger than the true ages of soils (**Wang et al., 1996**). Further complications might arise from the circulation of humic acids, roots penetration and earthworms and other biological activities. All of these make soil one of the most difficult of all materials to date using the radiocarbon technique (**Matthews, 2020**). Nevertheless, buried soils (paleosols) are important components of the Quaternary stratigraphic record. Thus, the result of the radiocarbon dating of this study can still be a useful approach to confirm the Holocene faulting activity and to estimate the minimal age constrain of the most recent surface-rupturing earthquake in the Haramachi segment.

Currently, the most reliable study that has claimed to have a bracket on the timing of the most recent event of the Haramachi segment was done by **Fukushima-ken (1999)**, who collected many ^{14}C dates from almost all of the sediment layers in a trenching wall conducted in the Mano River region. The authors estimation of the most recent event in the Haramachi segment was around 2,200-1,900 BP. However, this study has confirmed further the most recent event of the Haramachi segment with broader region coverage and improved the radiocarbon dating result.

The high-resolution remote sensing data supported by field evidence conducted in this study has produced the new estimation of the total length of the Haramachi segment which is about 25 km that extends from Hatsuno in Soma City to near the Yokokawa Dam in Minamisoma City. This length estimation is different from the previous study. However, the estimation result of this study is more reliable due to the high-quality material and new method approach. The difference is mainly due to the determination of active fault boundaries between researchers, which indirectly depends on the material used by each researcher.

Based on the empirical relationship between the surface rupture length and the moment magnitude (**Wells and Coppersmith, 1994**), the magnitude-seismic moment relation for the shallow earthquakes inland Japan (**Takemura, 1990**), and Matsuda's Equation (**Matsuda, 1975**); the Haramachi Fault segment is capable of producing Mw 6.5 - 7.0 or MJMA 7.2 earthquake if the active section of 25 km long ruptured altogether in the future.

8. Conclusion

The surface expression associated with recent faulting events supported by fault outcrop evidence in the field, suggests that the Haramachi segment deformation is distributed more complex to its northern terminus and forming horsetail splay fault geometry; confirming the fault tip termination characteristics.

The Quaternary activity of the Haramachi segment is confirmed by the evidence of geomorphic features observed in the field and remote sensing dataset. Systematic bending of the drainage pattern at the eastern foot of the Shiode Mountain characterizes the sinistral NNW-trending strike-slip fault mechanism. The lowest terrace surface deposited at the Uda River bank is interpreted to have been preserved as evidence for the most recent surface rupturing event on the Haramachi segment. The fault trace is thought to cut the lowest terrace surface which has been abandoned around 3900 cal BP based on the dated soil organic material obtained from the borehole survey on the terrace tread. The age then gives us a constraint that the most recent event occurred sometime after 3.9 ka in the Haramachi segment.

The high-resolution remote sensing data supported by field evidence has produced the new estimation of the total length of the Haramachi segment which is about 25 km. This fault segment is capable of producing earthquakes with a maximal moment magnitude (M_w) 6.5 - 7.0 or M_{JMA} 7.2. This estimation could be used for the refinement of the seismic safety evaluation, considering the relatively close proximity of the Haramachi segment of the Futaba Fault zone with the nuclear power plant sites.

Acknowledgement

We would like to thank Toshifumi Imaizumi (professor emeritus, Tohoku University) and Shinsuke Okada (Iwate University) for field assistance and supervising the study. We also thank the editor and reviewers for the constructive comments which improved the manuscript.

9. References

AFRG (Research Group for Active Fault of Japan). Active faults in Japan, new edition: Distribution map and the related materials. 437p, University of Tokyo Press, 1991.

AIST (National Institute of Advanced Industrial Science and Technology). Online active fault database of Japan. 2008.

Burbank, D. W., & Anderson, R. S. (2011): Tectonic geomorphology. John Wiley & Sons, 68-76.

Cunningham, W. D., & Mann, P. (2007): Tectonics of strike-slip restraining and releasing bends. Geological Society, London, Special Publications, 290(1), 1-12.

Fukushima-ken. (1999): Futaba fault survey, earthquake-related basic research grants FY 1998 report. Doc. 3826:109 p, http://www.hp1039.jishin.go.jp/danso/Fukushima3Bfrm.htm.

Goto, H. (2016): Extensive Area of Topographic Anaglyphs Covering Inland and Seafloor Derived Using a Detailed Digital Elevation Model for Identifying Broad Tectonic Deformations. In Earthquakes, Tsunamis and Nuclear Risks: Prediction and Assessment Beyond the Fukushima Accident (p. 65-74). Tokyo: Springer Japan.

GSJ (Geological Survey of Japan). Seamless digital geological map of Japan (1:200,000). https://www.jishin.go.jp/main/chousa/05apr futaba/index.htm.

Hall, M., Howard, A. S., Aspden, J., Addison, R., & Jordan, C. (2004): The use of anaglyph images for geological feature mapping.

HERP (Headquarters for Earthquake Research Promotion). (2005): Long Term Evaluation of Futaba Fault. https://www.jishin.go.jp/main/chousa/katsudansou_pdf/23_futaba.pdf

HERP (Headquarters for Earthquake Research Promotion). (2011): Long-Term Evaluation of Active Faults after the Offshore Pacific Tohoku Earthquake-Major active fault zones that may have high probability of earthquake occurrence. 12 p.

Kaneda, H., Goto, H., and Hirouchi, D. (2013): Active Fault Map in Urban Area, Futaba Fault Zone and its vicinity, Watari, Souma, Minamisouma (Scale 1:25,000) Reference Manual. Geospatial Information Authority of Japan. 17 p.

Kanisawa, S., Yoshida, T., Yokoyama, R., Sirasawa, M., Kikuchi, Y., & Ohguchi, T. (2000): Digital maps synthesized from 50m-mesh DEM:(2) Examples of typical geological information. In The Joint Meeting of Earth and Planetary Science.

Kato, A., Sakai, S. I., & Obara, K. (2011): A normal-faulting seismic sequence triggered by the 2011 off the Pacific coast of Tohoku Earthquake: Wholesale stress regime changes in the upper plate. Earth, planets and space, 63(7), 745-748.

Keller, E. A., Gurrola, L., & Tierney, T. E. (1999): Geomorphic criteria to determine direction of lateral propagation of reverse faulting and folding. Geology, 27(6), 515-518.

Keller, E.A. and Pinter, N. (2002): Active Tectonics, Earthquakes, Uplift and Landscape. 2nd Edition, Prentice Hall, Upper Saddle River, 362 p.

Kim, Y. S., Peacock, D. C., & Sanderson, D. J. (2004): Fault damage zones. Journal of structural geology, 26(3), 503-517.

Kubo, K., Yanagisawa, Y., Yamamoto, T., Komazawa, M., Hiroshima, T., & Sudo, S. (2003): Geological map of Japan 1: 200,000, Fukushima. Geological Survey of Japan.

Mann, P. (2007): Global catalogue, classification and tectonic origins of restraining-and releasing bends on active and ancient strike-slip fault systems. Geological Society, London, Special Publications, 290(1), 13-142.

Matthews, J. A. (2020): Radiocarbon dating of surface and buried soils: principles, problems and prospects. Geomorphology and soils, 269-288.

Matsuda, T. (1975): Magnitude and recurrence interval of earthquakes from a fault. Jour. Seism. Soc. Japan, 28, 269-287.

Matsumoto, H. (1976): Active Faults on the Northeastern Fringe of the Abukuma Mountains. Annals of the Tohoku Geographical Association, 28(3), 176-176.

Mori, N., Takahashi, T., Yasuda, T., & Yanagisawa, H. (2011): Survey of 2011 Tohoku earthquake tsunami inundation and run□up. Geophysical research letters, 38(7).

Nakata, T., & Imaizumi, T. (2002): Digital active fault map of Japan. 60p. https://gbank.gsj.jp/ld/resource/geolis/200203687.html

Otsuki, K. (1975): Geology of the Tanakura Shear Zone and adjacent area. Contributions from the institute of Geology and Paleontology, Tohoku Univ., 76, 1-72.

Otsuki, K. (1992): Oblique subduction, collision of microcontinents and subduction of oceanic ridge: their implications on the Cretaceous tectonics of Japan. Island Arc, 1(1), 51-63.

Otsuki, K., & Ehiro, M. (1992): Cretaceous left-lateral faulting in northeast japan and its bearing on the origin of geologic structure of japan. Journal of the Geological Society of Japan, 98(12): 1097-1112.

Patria, A., Tsutsumi, H., & Natawidjaja, D. H. (2021): Active fault mapping in the onshore northern Banda Arc, Indonesia: Implications for active tectonics and seismic potential. Journal of Asian Earth Sciences, 218, 104881.

Peacock, D. C. P., Nixon, C. W., Rotevatn, A., Sanderson, D. J., & Zuluaga, L. F. (2016): Glossary of fault and other fracture networks. Journal of Structural Geology, 92, 12-29.

Prima, O. D. A., & Yoshida, T. (2010): Characterization of volcanic geomorphology and geology by slope and topographic openness. Geomorphology, 118(1-2), 22-32.

Regalla, C., Fisher, D., & Kirby, E. (2010): Timing and magnitude of shortening within the inner fore arc of the Japan Trench. Journal of Geophysical Research: Solid Earth, 115(B3), 2-3.

Regalla, C., Kirby, E., Fisher, D., & Bierman, P. (2013): Active forearc shortening in Tohoku, Japan: Constraints on fault geometry from erosion rates and fluvial longitudinal profiles. Geomorphology, 195, 84-98.

Research Group for Active Faults of Japan. (1980): Active faults in Japan: sheet maps and inventories. 363p, University of Tokyo Press.

Research Group for Active Faults of Japan. (1991): Active faults in Japan, new edition: Distribution map and the related materials. 437p, University of Tokyo Press.

Sato, T. (2006). Anaglyph Images on Topography for Geographical Education. In Proceedings of the General Meeting of the Association of Japanese Geographers Annual Meeting of the Association of Japanese Geographers, Autumn 2006 (pp. 72-72). The Association of Japanese Geographers. https://user.numazu-ct.ac.jp/~tsato/tsato/graphics/anaglyph/process/process.html

Sato, H., Imaizumi, T., Yoshida, T., Ito, H., & Hasegawa, A. (2002). Tectonic evolution and deep to shallow geometry of Nagamachi-Rifu Active Fault System, NE Japan. Earth, planets and space, 54(11), 1039-1043.

Sato, H., Ishiyama, T., Kato, N., Higashinaka, M., Kurashimo, E., Iwasaki, T., & Abe, S. (2013, April). An active footwall shortcut thrust revealed by seismic reflection profiling: a case study of the Futaba fault, northern Honshu, Japan. In EGU General Assembly Conference Abstracts (pp. EGU2013-8117):

Simons, M., Minson, S. E., Sladen, A., Ortega, F., Jiang, J., Owen, S. E., ... & Webb, F. H. (2011): The 2011 magnitude 9.0 Tohoku-Oki earthquake: Mosaicking the megathrust from seconds to centuries. science, 332(6036), 1421-1425.

Suzuki, T., & Koarai, M. (1989): Outcrops and recent event of Futaba Fault (Ohgai Fault) at Kashima Town in Fukushima Prefecture, Northeast Japan. Act. Fault Res, 6, 23-29:

Suzuki, T., & Koarai, M. (1990): 14C Age of the Last Event along the Futaba (Ohgai) Fault at Kashima Town, Northeast Japan. Annals of the Tohoku Geographical Association, 42(1), 17-19.

Taira, A., Ohara, Y., Wallis, S. R., Ishiwatari, A., & Iryu, Y. (2016). Geological evolution of Japan: an overview. The geology of Japan, 1-24

Takemura, M. (1990): Magnitude-seismic moment relations for the shallow earthquakes in and around Japan. Zisin (J. Seism. Soc. Japan), 43, 257-265.

Toda, S., Lin, J., & Stein, R. S. (2011): Using the 2011 M w 9.0 off the Pacific coast of Tohoku Earthquake to test the Coulomb stress triggering hypothesis and to calculate faults brought closer to failure. Earth, planets and space, 63(7), 725-730.

Walker, M. (2005): Quaternary dating methods. John Wiley and Sons. 31.

Wang, Y., Amundson, R., & Trumbore, S. (1996): Radiocarbon dating of soil organic matter. Quaternary Research, 45(3), 282-288.

Wells, D. L., & Coppersmith, K. J. (1994): New empirical relationships among magnitude, rupture length, rupture width, rupture area, and surface displacement. Bulletin of the seismological Society of America, 84(4), 974-1002.

Yamamoto, T. (2005): The rate of fluvial incision during the Late Quaternary period in the Abukuma Mountains, northeast Japan, deduced from tephrochronology. Island Arc, 14(2), 199-212.

Yanagisawa, Y., Yamamoto, T., Banno, Y., Tazawa, J., Yoshioka, T., Kubo, K., & Takizawa, F. (1996): Geology of the Somanakamura district, 144 p. with Geological Sheet Map at 1: 50,000. Geological Survey of Japan. Tsukuba. In Japanese with English abstract.

Yeats, R.S., Sieh, K., Allen, C.R. (1997): The Geology of Earthquakes. Oxford University Press, New York.

Yokoyama, R., Shirasawa, M., & Pike, R. J. (2002): Visualizing topography by openness: A new application of image processing to digital elevation models. Photogrammetric engineering and remote sensing, 68(3), 257-266.

SAŽETAK

Kasno kvartarna aktivnost segmenta Haramachi Futaba rasjeda u sjeveroistočnom Japanu uočena na temelju topografskih anaglifskih slika i analize sedimenata jezgre bušotine

Segment rasjeda Haramachi, dio je Fatuba rasjedne zone u sjeveroistočnom dijelu Japanskog luka, na otoku Honshu. Segment rasjeda Haramachi ukazuje uglavnom na lijeve pomake rasjeda s manjom reversnom komponentom. Potres intenziteta 9,0 Mw dogodio se 2011. godine u blizini pacifičke obale Tohokua koji je izazvao velike deformacije kore. Unatoč tome što predstavlja aktivni rasjed najbliži epicentru, u zoni rasjeda Futaba provedena su vrlo ograničena istraživanja. U prethodnim istraživanjima korištene su topografske karte manjeg mjerila, dok je aktivnost rasjeda procijenjena samo na temelju istraživanja izrađenih rovova i bušotinskih podataka u središnjem dijelu segmenta rasjeda Haramachi. Stoga, geometrija, kinematika, kao i nedavna tektonska aktivnost segmenta rasjeda nije dobro identificirana, osobito u sjevernom dijelu. U ovom istraživanju korištena je kombinacija DEM-ova visoke razlučivosti (mreža od 2 m i 5 m), nekoliko vrsta topografskih anaglifskih prikaza (nagib, negativna i pozitivna otvorenost), kao i terensko istraživanje kako bi se potvrdila interpretacija podataka dobivenih daljinskim istraživanjima. Neznantne površinski izražene deformacije povezane s aktivnim rasjedanjem, kao što su izdignute deformirane terase, pomaknute drenaže i mali pomaci rasjeda vidljivi na površini mogu se sada jasnije identificirati. Nedavna aktivnost rasjednog sustava vidljiva je kroz identifikaciju nekoliko novih rasjeda, čije je postojanje potkrijepljeno rezultatima terenskih istraživanja. Nova procjena ukupne duljine Haramachi segmenta dobivena pristupom iz ovog istraživanja iznosi 25 km, što može proizvesti potres od 6,5 – 7,0 Mw ili 7,2 Mjma. Štoviše, ispitivanje plitkih bušotina i datiranje ugljika iz organskog materijala tla otkrilo je minimalnu vremensku procjenu najnovijeg rasjedanja u Haramachi segmentu na 3694 ± 24 BP. Ovaj pristup revidirao je razumijevanje aktivne distribucije rasjeda i deformacija povezanih s Haramachi segmentom i potvrdio vrijeme najnovijeg događaja rasjedanja u širem smislu.

Ključne riječi:
kasno kvartarna aktivnost; segment Haramachi; rasjedna zona Futaba; sjeveroistočni Japan

Author Contribution

Anggraini Rizkita Puji (1) (Junior Researcher, Tectonic Geomorphology / Active Tectonic) provided the conceptualization of the research, tectonic geomorphology interpretation, performed the field work, sedimentation phase analysis, and presentation of the results in the manuscript. Naoya Takahashi (2) (Assistant Professor, Tectonic/Fluvial geomorphology / Earthquake geology,) performed the field work, calculated the calibrated age of radiocarbon dating results, provided the seismicity data from JMA, improved the manuscript. Shinji Toda (3) (Professor, Active Fault / Inland Earthquake / Seismicity / Earthquake Probability) contributed with the refinement of tectonic geomorphology interpretation, supervised the field work result, and contributed by improving the manuscript quality.